Nonlinear self-excited forces on a 5:1 rectangular cylinder in torsional post-flutter

Chaoqun Wang [1,2], Tommaso Massai [2], Niccolò Barni [2], Xugang Hua [1,*], Claudio Mannini [2,*]

[1]*Key Laboratory for Wind and Bridge Engineering of Hunan Province, College of Civil Engineering, Hunan University, Changsha, China, cexghua@hnu.edu.cn*
[2]*CRIACIV / Department of Civil and Environmental Engineering, University of Florence, Florence, Italy, claudio.mannini@unifi.it*

SUMMARY:
A series of aeroelastic wind tunnel tests were carried out on the section model of a 5:1 rectangular cylinder, to study the self-excited forces during post-flutter oscillations. Great care was devoted to realize perfectly synchronous measurements of model displacement and aerodynamic pressures. Both limit-cycle oscillations and transient response were considered. Amplitude-dependent flutter derivatives were also obtained and discussed. Nonlinearity and unsteadiness of the self-excited forces were preliminary analysed based on hysteresis loops.

Keywords: post-flutter, nonlinear self-excited force, 5:1 rectangular cylinder

1. INTRODUCTION

In the last decades, great attention has been paid to the nonlinear post-flutter behaviour of slender structures, especially for energy harvesting applications (Pigolotti et al., 2017) and in bridge engineering (Wu et al., 2011). In the post-flutter state, self-excited forces present strong nonlinear features and exhibit hysteresis loops, which play an essential role in the structural response (Diana, et al., 2008). Therefore, the measurement and mathematical modelling of these nonlinear forces are crucial topics in bridge aerodynamics nowadays. Along this line, in this work wind tunnel tests pivoting on synchronous displacement and pressure measurements were carried out on a 5:1 rectangular cylinder.

2. OUTLINE OF WIND TUNNEL TEST

A section model of a 5:1 rectangular cylinder, with cross-section dimensions 0.25 m×0.05 m and a length of 1.2 m, was employed for the aeroelastic tests in the CRIACIV wind tunnel at the University of Florence. 64 pressure taps were arranged in the middle-span cross section of the model (Fig. 1). Two clock springs were installed at the two ends of the model to realize a single-degree-of-freedom (torsional) system enabling large oscillations without significant structural nonlinearities (Fig. 2). The mass moment of inertia of the model was $J = 2.06\times10^{-2}$ Kg·m^2/m, the natural frequency was $f_{\alpha 0}$ = 6.98 Hz, and the structural damping was $\xi_{\alpha 0}$ = 0.8-1.3% (decreasing with the vibration amplitude, in the range concerned in this study). An electrical trigger was realized for the synchronous sampling of displacement and pressure data, carefully considering all possible sources of time delay in the measurements. A null wind angle of attack ($\alpha = 0°$) was considered in all tests.

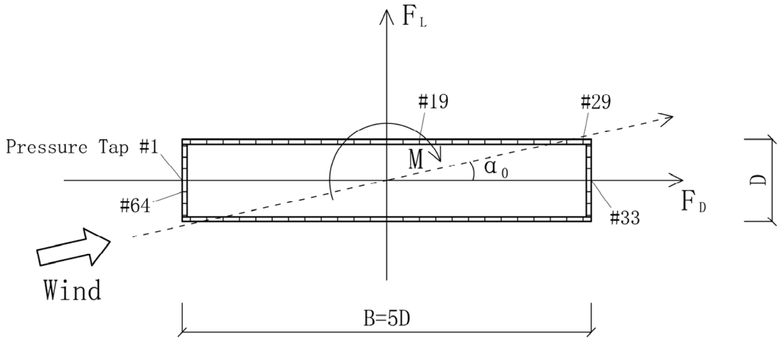

Figure 1. Cross section of the 5:1 rectangular cylinder.

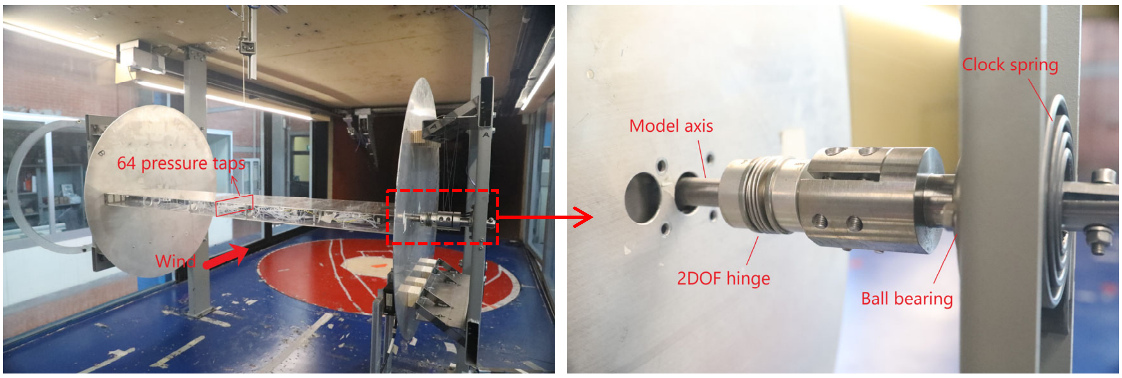

Figure 2. View of the rectangular cylinder model installed in the wind tunnel setup.

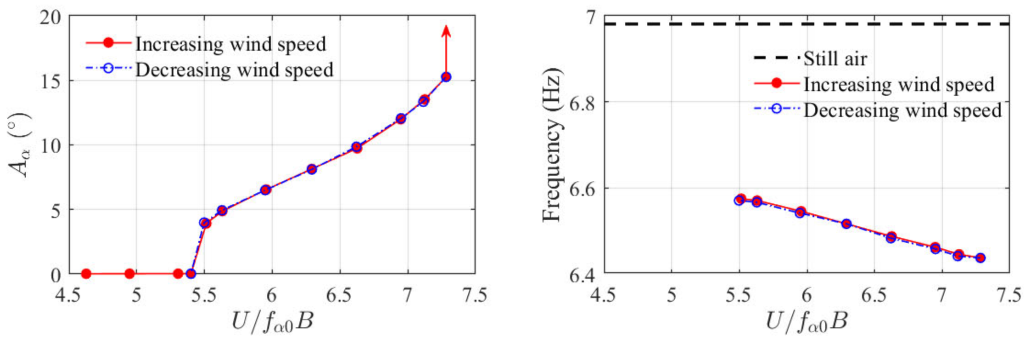

Figure 3. LCO response of the model.

3. TEST RESULTS

3.1. Post-flutter behaviour

Limit-cycle oscillation (LCO) amplitude and corresponding vibration frequency against wind speed are shown in Fig. 3 (U denotes the wind speed, B the model width, and A_α the oscillation amplitude). The vibration amplitude increases with the wind speed and a jump to a catastrophic branch is encountered around $U/f_{\alpha 0}B = 7.3$. No hysteresis is observed in the post-critical oscillations in the range $5.5 \leq U/f_{\alpha 0}B \leq 7.3$. Moreover, noteworthy is the non-negligible decrease of the torsional frequency in the same wind speed range.

3.2. Nonlinear self-excited forces

Based on a series of free-decay and build-up tests, the four flutter derivatives A_2, A_3, H_2, and H_3, were obtained for different oscillation amplitudes and compared with previous results of Matsumoto et al. (1996), as shown in Fig. 4 (where f_α this time is the vibration frequency under wind). In general, the results at small vibration amplitude agree well with the previous ones, indicating the reliability of the measurements in the current study.

Fig. 4 clearly shows that all the flutter derivatives associated with the torsional motion are significantly affected by the vibration amplitude, that is, the aerodynamic damping and stiffness of the model quickly vary with the vibration amplitude, which is the main cause of the relatively low amplitude LCOs observed in the experiments.

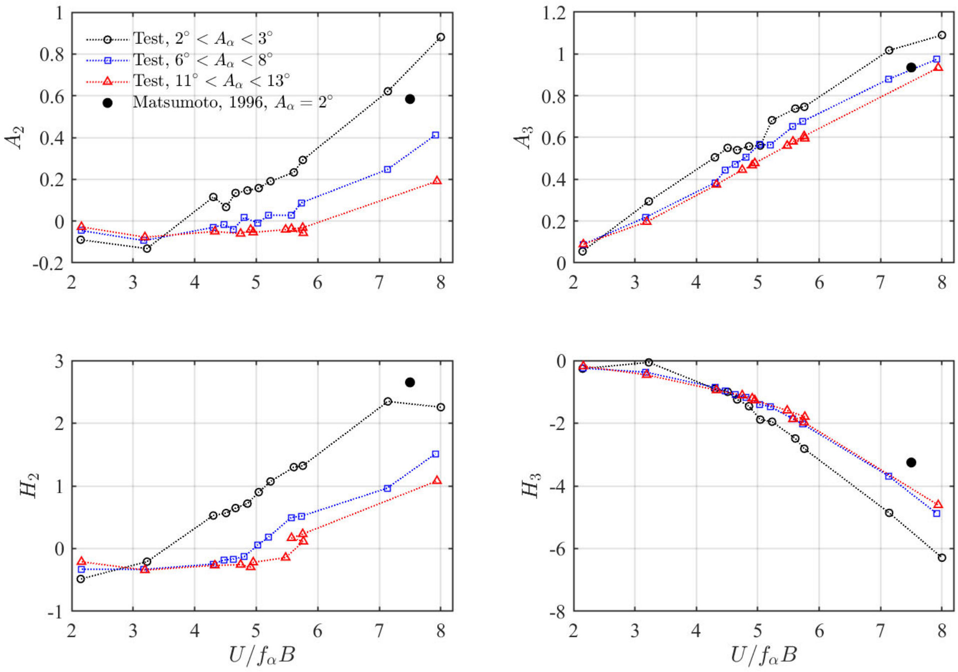

Figure 4. Flutter derivatives as a function of oscillation amplitude.

Hysteresis loops of the aerodynamic force coefficients at three reduced wind speeds (associated with different LCO amplitudes, see Fig. 3), as well as the corresponding fits based on 7th-order Fourier series, are depicted in Fig. 5. The static force coefficient curves are also shown for comparison. Both lift and moment present significant hysteretic and nonlinear characteristics. Specifically, despite the clear unsteady effects, the hysteresis loops of the lift force roughly follow the static curves for $A_\alpha < 7.5°$, but they maintain a positive slope (though with lower gradients) also for $7.5° < A_\alpha < 12.5°$. In contrast, the hysteresis loops of the aerodynamic moment exhibit an opposite behaviour compared to the static coefficients for $A_\alpha < 4°$, and the same trends but with higher slopes for larger oscillation amplitudes. These features of the self-excited forces suggest that the massive separation associated with the burst of the separation bubbles on the upper and lower sides of the cylinder are significantly delayed due to the torsional motion. Though not reported here in the interest of brevity, this behaviour is confirmed by first- and second-order moment statistics of the pressure coefficients, which show patterns qualitatively similar to those observed in turbulent flow (Mannini et al., 2017).

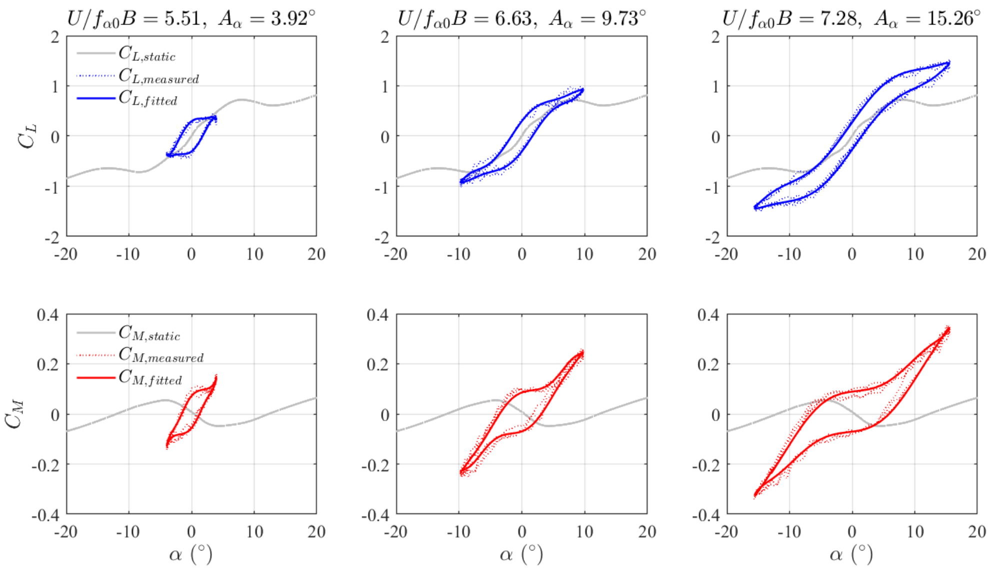

Figure 5. Hysteresis loops of aerodynamic forces.

6. CONCLUSION

Torsional LCO amplitudes of the 5:1 rectangular cylinder were found to increase gradually with the wind speed and then jump to very large values. The self-excited forces present strong unsteady and nonlinear features in the post-flutter non-catastrophic regime.

ACKNOWLEDGEMENTS

This study is sponsored by the National Science Foundation of China (No. 52025082) and China Scholarship Council (No. 202006130089), which are gratefully acknowledged.

REFERENCES

Diana, G., Resta, F., Rocchi, D., 2008. A new numerical approach to reproduce bridge aerodynamic non-linearities in time domain. Journal of Wind Engineering and Industrial Aerodynamics 96, 1871–1884.

Mannini, C., Marra, A. M., Pigolotti, L., Bartoli, G., 2017. The effects of free-stream turbulence and angle of attack on the aerodynamics of a cylinder with rectangular 5:1 cross section. Journal of Wind Engineering and Industrial Aerodynamics 161, 42–58.

Matsumoto, M., 1996. Aerodynamic damping of prisms. Journal of Wind Engineering and Industrial Aerodynamics 59, 159–175.

Pigolotti, L., Mannini, C., Bartoli, G., 2017. Experimental study on the flutter-induced motion of two-degree-of-freedom plates. Journal of Fluids and Structures 75, 77–98.

Wu, T., Kareem, A., 2011. Modeling hysteretic nonlinear behavior of bridge aerodynamics via cellular automata nested neural network. Journal of Wind Engineering and Industrial Aerodynamics 99, 378–388.